Int. J. Multiphase Flow Vol. 16, No. 5, pp. 899–907, 1990
Printed in Great Britain.

0301-9322/90 $3.00 + 0.00

WALL-INDUCED LIFT ON A SPHERE

P. CHERUKAT and J. B. MCLAUGHLIN†
Department of Chemical Engineering, Clarkson University, Potsdam, NY 13676, U.S.A.

(*Received* 6 *November* 1989; *in revised form* 1 *April* 1990)

Abstract—The lateral migration of rigid spheres sedimenting near a large flat vertical wall, in a quiescent Newtonian fluid, has been studied experimentally. The migration velocities were measured by recording the trajectory of the spheres as they sedimented near a wall for the particle Re range 0.1–10.0. The measurements indicate that the expression derived by Vasseur & Cox [*J. Fluid Mech.* **80**, 561–591 (1977)] predicts, fairly accurately, the migration velocity up to a particle Re of 3.0.

Key Words: inertia, lateral, lift, migration, sedimentation, wall

1. INTRODUCTION

A rigid sphere, sedimenting near a flat vertical wall in a quiescent Newtonian fluid migrates away from the wall (i.e. experiences a lift) as it settles. Creeping flow equations are time reversible; hence these equations predict zero migration velocity for a sphere sedimenting near a flat vertical wall. It is also been shown mathematically by Saffman (1956) and Bretherton (1962) that the solution of the Navier–Stokes equations predicts zero migration velocity if the inertial terms are not considered. Hence the observed lateral migration of sedimenting spheres is an inertial effect. Cox & Brenner (1968) and Cox & Hsu (1977) derived expressions for the migration velocity of a rigid sphere sedimenting in a quiescent fluid near a flat wall by the method of matched asymptotic expansions. In these analyses, it was assumed that the wall lies in the inner region. Vasseur & Cox (1977) generalized the analysis, to allow for the possibility that the wall could be in the outer region, and obtained an expression for the migration velocity. These authors also measured the migration velocities of sedimenting spheres by tracking spherical resin particles of dia 0.627–1.11 mm sedimenting in aqueous glycerol, near a flat vertical wall. The Reynolds number (Re) based on the diameter of the sphere was in the range 0.026–0.26.

In this paper, we present new experimental measurements of migration velocity and compare them with the prediction by Vasseur & Cox (1977). The Re values investigated in this study were in the range 0.1–10.0.

One of the motivations for the present study was a computer simulation of aerosol deposition in a turbulent channel flow (McLaughlin 1989), which indicated that the aerosols which deposit develop Re values of order unity as they pass through the viscous sublayer. The cause of the large particle Re is the combination of their own inertia and the large normal gradient of the mean streamwise component of fluid velocity near the wall. To a good approximation, the particles move parallel to the wall through a (nearly) stagnant fluid. There is a need for quantitative information about the lift acting on such particles when their Re is not small compared to unity.

2. MEASUREMENT OF LIFT VELOCITY

A schematic of the apparatus used for studying the wall-induced migration on rigid spheres is shown in figure 1. It consists of a (108 × 108 × 200 mm) cell made of a 6.35 mm Plexiglas sheet, mounted on an optical rail, two video cameras (A and B) having zoom lenses mounted on another optical rail, a video synchronizer-cum-timer, a video cassette recorder (VCR), a video monitor, an X–Y indicator and an IBM PC with a 12-bit A/D converter board. The outputs from video cameras A and B are composed into a single composite split-screen image by the video synchronizer, so

†To whom all correspondence should be addressed.

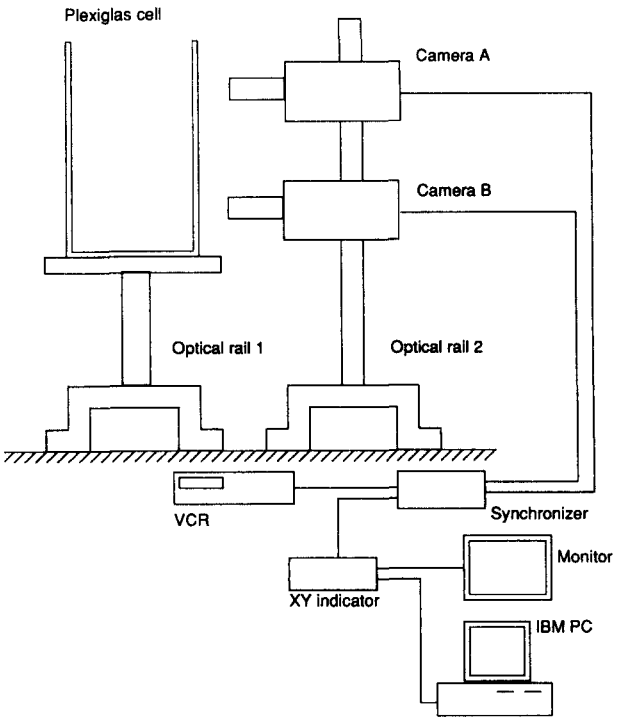

Figure 1. Experimental setup for measuring the wall-induced migration velocity.

that the field of view of camera A is displayed on the upper half of the video monitor screen and that of camera B is displayed on the lower half of the screen. The synchronizer also identifies and numbers each frame. The composite image is recorded by the VCR. The input to the $X-Y$ indicator can be either a video signal from the VCR or a video signal from the synchronizer. The $X-Y$ indicator generates an output video signal by superimposing vertical and horizontal cross-hair images on the input signal. This output signal can be displayed on the video monitor. The vertical and horizontal cross hairs can be positioned anywhere on the monitor screen. The $X-Y$ indicator also generates analog signals whose values depend on the positions of the cross hairs on the monitor screen. These analog signals are digitized and sampled by the 12-bit A/D converter. The digitizing and sampling of these analog signals are controlled by a computer program running on the IBM PC.

The vertical alignment of the cameras and the cell walls is very crucial in accurately measuring the migration velocity. Cameras A and B were focused on a plumb line made of 0.1 mm platinum wire and the image of the plumb line with vertical and horizontal cross hairs superimposed on it was displayed on the video monitor screen. The leveling screws on the base of the optical rail, on which the cameras were mounted, were adjusted until the image of the plumb line, on the video monitor, became parallel to the vertical cross hair. This ensured that the cameras were properly aligned (i.e. the image of any vertical line would appear vertical on the monitor screen). The Plexiglas cell was placed on the platform and the cameras were focused on one of the edges of the cell. The leveling screws on the base of the optical rail on which the platform was mounted were adjusted until the image of this edge, on the monitor screen, became parallel to the vertical cross hair. Since the cameras had been aligned properly this ensured that the cell walls were vertically aligned (i.e. the platform was horizontal).

Figure 2 shows the top view of the Plexiglas cell and the cameras. The Plexiglas cell was placed on the platform in such a way that one of the vertical walls (W2W3) was parallel to the focal planes of the camera lenses and the field of view of each camera was a small region near the wall W1W2. The cell was then filled with Dow Corning 200 fluid (silicone oil). The plumb line was inserted in the cell so that it passed through a point on the F1F2 plane close to the wall. The cameras were focused so that a clear image of the plumb line appeared on the monitor screen and this image was recorded. The distance of the plumb line from the wall W1W2 was measured carefully. This

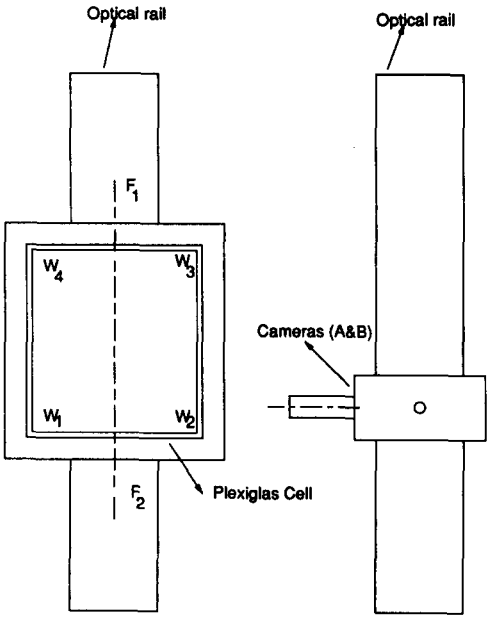

Figure 2. Top view of the Plexiglas cell and the cameras.

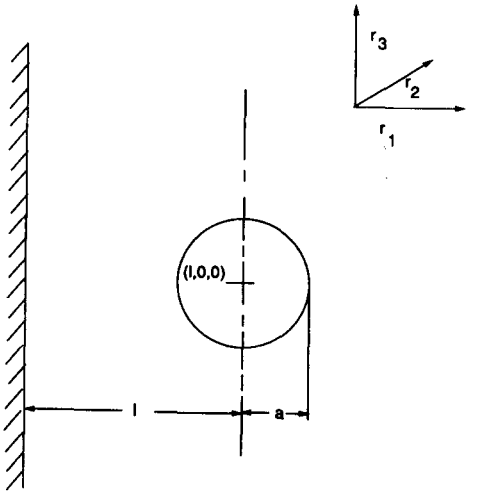

Figure 3. Coordinate system for a sedimenting sphere.

image was used as a reference distance from the wall to determine the distance of any point on the F1F2 plane from the wall W1W2. A flat graduated scale was placed so that it coincided with the plane F1F2 and its image was recorded. The vertical cross hair was positioned at different graduations on the image of the scale and the values of the corresponding analog signals were noted. From these observations, the change in the value of the analog signal per unit distance in the F1F2 plane was determined by linear regression. The horizontal distance between any point on the F1F2 plane and the wall W1W2 could be determined from the value of an analog signal when the vertical cross hair was positioned on the image of that point and the value of the analog signal when the vertical cross hair was positioned on the image of the plumb line.

A plastic sphere was released at a point on the F1F2 plane close to the wall W1W2. The images of the sphere at two instants as it sedimented were recorded by cameras A and B. The video tape was played back and the frame corresponding to the instant when the sphere was in the field of view of camera A was displayed on the screen. The vertical cross hair was aligned with the edge of the sphere and the analog signal corresponding to this position of the vertical cross hair was sampled and the frame number was noted. Then the frame corresponding to the instant when the sphere was in the field of view of camera B was displayed on the screen and the analog signal corresponding to the position of the vertical cross hair when it was aligned with the edge of the sphere was sampled and the frame number was noted. The average migration velocity was calculated by dividing the horizontal distance traveled by the sphere by the elapsed time.

These experiments were done with different grades of Dow Corning 200 fluid (kinematic viscosities—0.1×10^{-4}, 0.5×10^{-4}, 1.0×10^{-4} and 2.0×10^{-4} m^2/s; and densities—935.0, 949.0, 960.0, 964.0 and 967.0 kg/m^3, respectively) and polymethyl methacrylate (PMMA) and polystyrene spheres of different diameters (2, 3, 3.175, 5.0 and 6.35 mm). The viscosity of the liquid was measured with a Brookfield viscometer. The density of the liquid was determined by weighing a known volume of the liquid.

3. COMPARISON OF THE EXPERIMENTAL DATA WITH THEORETICAL MODELS

Consider a sphere, of radius a, sedimenting in a quiescent fluid near a flat infinite wall, as shown in figure 3. The settling velocity of the sphere is $-\hat{\mathbf{e}}_3 V_s$ and the migration velocity of the sphere is $\hat{\mathbf{e}}_1 V_m$, where $\hat{\mathbf{e}}_1$, $\hat{\mathbf{e}}_2$ and $\hat{\mathbf{e}}_3$ are the unit basis vectors in the r_1, r_2 and r_3 directions, respectively.

The position vector of the center of the sphere is denoted by $\mathbf{r}^*$ and has components $(l, 0, 0)$. The Re based on the diameter of the sphere is defined by

$$\mathrm{Re}_p = \frac{2aV_s}{\nu}, \qquad [1]$$

and the Re based on the distance of the center of the sphere from the wall l is defined by

$$\mathrm{Re}_l = \frac{lV_s}{\nu}, \qquad [2]$$

where ν is the kinematic viscosity. The quantity κ is the ratio of the radius of the sphere to the distance between the center of the sphere and the wall, i.e.

$$\kappa = \frac{a}{l}. \qquad [3]$$

As mentioned in section 1, it is necessary to consider the inertial terms in the Navier–Stokes equations to obtain a nonzero migration velocity for a sphere sedimenting near a flat wall. Cox & Brenner (1968), considered the general problem of lateral migration of particles of arbitrary shape in a fluid undergoing Poiseuille flow and bounded by a system of walls. An expression for the lateral migration to $O(\mathrm{Re}_p)$, was derived by the method of matched asymptotic expansions. It was assumed that the inequality

$$\mathrm{Re}_p \ll \kappa \ll 1 \qquad [4]$$

is satisfied. This implies that the wall lies in the inner region where viscous effects are predominant. If the undisturbed flow field is $O(r^m)$ and the zeroth-order disturbance field (creeping flow solution) is $O(r^{-n})$ as $r \to \infty$, then, if $n > m + 1$, it can be shown that the $O(\mathrm{Re}_p)$ velocity field in the inner region can be obtained without considering an outer expansion. In the case of a sphere sedimenting near a flat wall, the creeping flow solution is $O(r^{-2})$ as $r \to \infty$. The expression for the migration velocity obtained by these authors was

$$V_m = \frac{6\pi a V_s^2}{\nu} h + o(\mathrm{Re}_p), \qquad [5]$$

where h is given by

$$h = \int_{-\infty}^{\infty}\int_{-\infty}^{\infty}\int_{0}^{\infty} V_{i1}\frac{\partial V_{i2}}{\partial r_2}\,dr_1\,dr_2\,dr_3. \qquad [6]$$

In [6], V_{ij} is a Green's function for creeping flow satisfying the equations

$$\frac{\partial^2 V_{ij}}{\partial r_k \partial r_k} - \frac{\partial P_j}{\partial r_i} + \delta_{ij}\delta(\mathbf{r} - \mathbf{r}^*) = 0, \qquad [7]$$

$$\frac{\partial V_{ij}}{\partial r_i} = 0, \qquad [8]$$

$$V_{ij} = 0 \quad \text{at } r_1 = 0 \qquad [9]$$

and

$$V_{ij} = 0 \quad \text{as } r \to \infty. \qquad [10]$$

Here δ_{ij} is the Kronecker delta and δ is the Dirac delta function.

Cox & Hsu (1977) evaluated the intergral h in [6] by determining the Green's function for a point force in a quiescent fluid near a flat wall. The value of the integral was found to be $1/(64\pi)$. Thus, the expression for the migration velocity of a sphere sedimenting near a flat wall in a quiescent fluid is

$$V_m = \frac{3}{64}\mathrm{Re}_p V_s + o(\mathrm{Re}_p). \qquad [11]$$

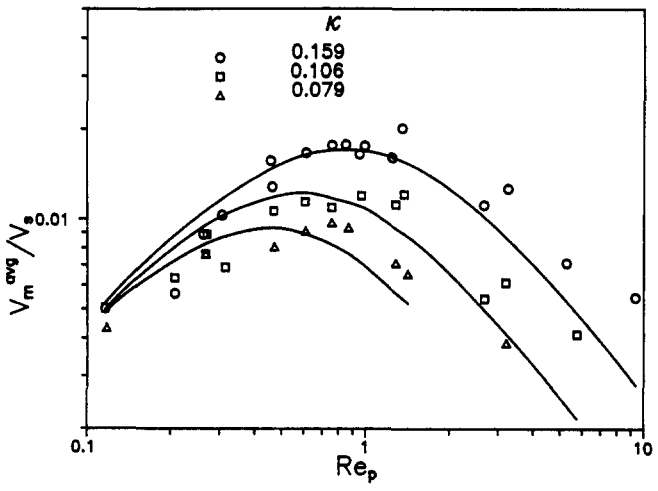

Figure 4. Plot of V_m^{avg}/V_s vs Re_p.

It can be seen from this expression that the migration velocity of a sphere sedimenting at a constant velocity, does not depend on the distance from the wall, when the wall is in the inner region. Figure 4 shows the plots of the ratio V_m^{avg}/V_s vs Re_p, for three different values of the ratio κ. Here V_m^{avg} is the average migration velocity and κ corresponds to the initial position of the sphere (i.e. corresponding to the image recorded by camera A, as described in section 2). It can be seen from these plots that the ratio V_m^{avg}/V_s does depend on the position of the sphere from the wall for the values of κ considered in this experimental study.

Vasseur & Cox (1977) generalized the analysis of Cox & Hsu (1977) by using an Oseen approximation for the nonlinear term in the Navier–Stokes equations. By this technique, they were able to remove the restriction $Re_l \ll 1$, although, like Cox & Hsu, they assumed that $Re_p \ll 1$. By considering the Oseen form for the disturbance due to a point force located at $(l, 0, 0)$ and the disturbance due to the wall at this point, these authors derived an expression for the force acting on the sphere. To the lowest order, the migration velocity was obtained by equating the r_1 component of the force to the Stokes drag. The expression for the migration velocity of the sphere was

$$V_m = \frac{3va}{4\pi l^2} I + o(Re_p), \qquad [12]$$

where I is a dimensionless integral given by

$$I = \int_0^\infty \int_0^{2\pi} \frac{q+s}{q-s} (e^{-s} - e^{-q}) s \, ds \, d\phi, \qquad [13]$$

and

$$q^2 = s^2 + iRe_l \cos\phi. \qquad [14]$$

The asymptotic limits for [12] are

$$V_m = \frac{3}{64} Re_p V_s \quad \text{for } Re_l = 0 \qquad [15]$$

and

$$V_m = \frac{3va}{8l^2} \qquad \text{for } Re_l = \infty. \qquad [16]$$

It should be noted that [15] has the same form as Cox & Hsu's (1977) expression [11] for the migration velocity.

The experiment described in section 2 enables one to determine the average migration velocity V_m^{avg} of the sphere. If the sphere moves from a distance l_1 from the wall to a distance l_2 from the wall in time T, then the average migration velocity over time T is given by

$$V_m^{avg} = \frac{(l_2 - l_1)}{T}. \quad [17]$$

The average migration velocity over a time interval T, predicted by the theory of Vasseur & Cox (1977) was computed by simulating the trajectory of the sphere. The distance traveled in the horizontal direction by the sphere in time T was computed by solving the initial-value problem

$$\frac{dl}{dt} = \frac{3va}{4\pi l^2} I, \quad [18]$$

$$l = l_1 \quad \text{at } t = 0. \quad [19]$$

This initial-value problem was solved by a fourth-order Runge–Kutta scheme. The double integral I was computed numerically after transforming it into the definite integral

$$I = -\int_0^1 \int_0^{2\pi} \frac{q - \ln p}{q + \ln p} (p - e^{-q}) \ln p \frac{dp}{p} d\phi. \quad [20]$$

In all the trajectory simulations the value of l_1 was the same as in the corresponding experiment and T was the time interval determined experimentally. It was also assumed that the variation of settling velocity over a distance $(l_2 - l_1)$ due to wall effects is negligible.

The experimentally determined average migration velocity and the average migration velocity predicted by [12] are compared by plotting the ratio of these two quantities vs Re_p. Figure 5 shows this plot. It can be seen that the migration velocities predicted by Vasseur & Cox's (1977) theory agree very well with the experimentally determined migration velocities up to $Re_p = 3.0$, especially for low values of κ (κ is based on the initial position of the center of the sphere); i.e. at large distances from the wall. The experimentally determined average migration velocities and the corresponding theoretically predicted values and the errors in the predicted values are given in table 1 (a–f). Figure 6 shows the plot of $V_m/(V_s Re_p)$ vs Re_f. This plot indicates that the ratio $V_m/(V_s Re_p)$ reaches an asymptotic value as Re_f becomes small, but not in agreement with Vasseur & Cox (1977).

Vasseur & Cox (1977) showed that a sphere sedimenting in a stagnant fluid near a large flat wall does rotate to $O(Re_p)$. The rotation of the spheres in the experiments described in this paper was studied by painting a mark on the surface and observing the position of the mark as the spheres sedimented. No rotation was observed—even when the centers of the spheres were as close as 2 radii from the wall. Rotation of the spheres was observed only when the spheres touched the wall. In this case it appeared as though the spheres rolled down the wall without migrating laterally.

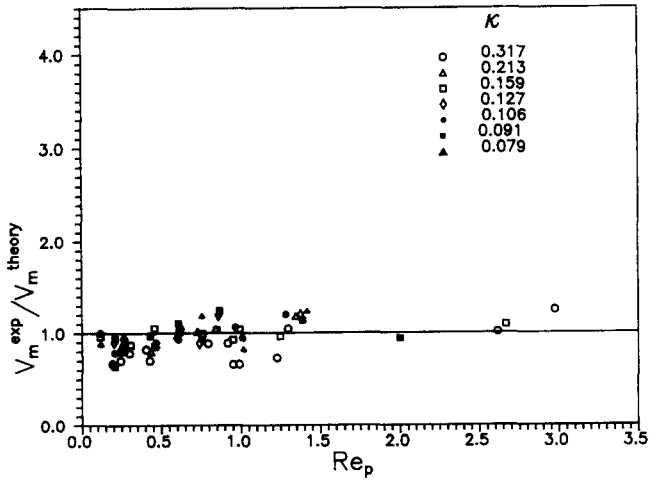

Figure 5. Plot of the ratio of the measured migration velocity (○) to the value predicted by Vasseur & Cox's (1977) expression (——), vs Re_p.

Table 1. Measured migration velocities and the migration velocities predicted by Vasseur & Cox's (1977) expression for the Re_p range 0.1–3.0

Dia (mm)	$\nu \times 10^{-4}$ (m^2/s)	Re_p	V_m^{avg}(mm/s): experimental	V_m^{avg}(mm/s): Vasseur & Cox (1977) theory	$\frac{\lvert V_m^{exp} - V_m^{theory} \rvert}{V_m^{exp}} \times 100$
		(a) $\kappa = 0.317$; r.m.s. error $\times$ 100 = 30.6			
3.000	1.046	0.243	0.064	0.092	43.7
3.000	0.549	0.950	0.304	0.462	51.9
3.000	0.564	0.918	0.403	0.454	12.6
3.000	0.604	0.794	0.353	0.400	13.3
3.175	0.337	1.297	0.402	0.385	4.2
6.350	0.539	2.976	0.852	0.681	20.0
6.350	1.025	0.989	0.306	0.464	51.6
3.175	0.723	0.248	0.050	0.062	24.0
3.175	0.549	0.427	0.090	0.129	43.3
3.175	0.232	2.615	0.099	0.120	21.2
5.000	2.119	0.299	0.129	0.166	28.7
5.000	1.023	1.226	0.641	0.749	16.8
2.000	0.118	5.882	0.530	0.457	13.8
		(b) $\kappa = 0.213$; r.m.s. error $\times$ 100 = 13.8			
2.000	0.210	3.850	0.439	0.374	14.8
3.000	0.832	0.434	0.154	0.193	25.3
3.175	0.337	1.346	0.354	0.300	15.3
3.175	0.722	0.265	0.065	0.068	4.6
3.000	0.708	0.600	0.245	0.251	2.4
3.000	0.603	0.843	0.371	0.355	4.3
		(c) $\kappa = 0.159$; r.m.s. error $\times$ 100 = 11.1			
3.000	0.646	0.759	0.277	0.279	0.7
3.000	0.606	0.850	0.303	0.294	3.0
3.175	0.337	1.355	0.290	0.225	22.4
3.175	0.232	2.667	0.217	0.198	8.8
3.175	0.549	0.462	0.102	0.120	17.6
6.350	1.025	0.951	0.257	0.277	7.8
3.175	1.046	0.166	0.019	0.020	5.3
3.175	0.549	0.457	0.124	0.177	5.6
3.000	1.046	0.261	0.081	0.096	18.5
3.000	0.549	0.992	0.318	0.306	3.8
3.000	0.709	0.614	0.242	0.239	1.2
5.000	1.057	1.247	0.422	0.436	3.3
5.000	2.119	0.306	0.134	0.154	14.9
		(d) $\kappa = 0.106$; r.m.s error $\times$ 100 = 14.9			
3.000	0.549	1.011	0.188	0.200	6.4
3.000	1.046	0.267	0.071	0.089	25.3
3.000	0.549	0.994	0.261	0.198	24.1
3.000	0.713	0.608	0.165	0.177	7.3
3.175	1.046	0.116	0.019	0.019	—
6.350	1.026	0.965	0.186	0.175	5.9
3.175	0.319	1.376	0.167	0.123	26.3
3.175	0.232	2.680	0.107	0.096	10.3
3.175	0.549	0.468	0.086	0.096	11.6
3.175	0.723	0.270	0.054	0.059	9.3
3.000	0.646	0.757	0.178	0.191	7.3
		(e) $\kappa = 0.091$; r.m.s. error $\times$ 100 = 10.8			
0.2000	0.211	2.000	0.095	0.101	6.3
0.3000	0.604	0.868	0.202	0.162	19.8
0.3000	0.713	0.608	0.166	0.150	9.7
0.3000	0.849	0.431	0.123	0.127	3.3
0.3175	0.319	1.389	0.108	0.095	12.0
0.3175	0.832	0.208	0.040	0.042	5.0
		(f) $\kappa = 0.079$; r.m.s. error $\times$ 100 = 16.1			
5.0000	1.025	1.282	0.187	0.149	20.3
3.0000	0.549	1.016	0.105	0.127	20.9
3.0000	1.047	0.267	0.071	0.077	8.5
3.1750	0.549	0.470	0.065	0.076	16.9
3.1750	1.047	0.117	0.017	0.019	11.8
3.1750	0.319	1.418	0.093	0.075	19.4
3.0000	0.713	0.610	0.132	0.129	2.3
3.0000	0.604	0.868	0.163	0.133	8.4

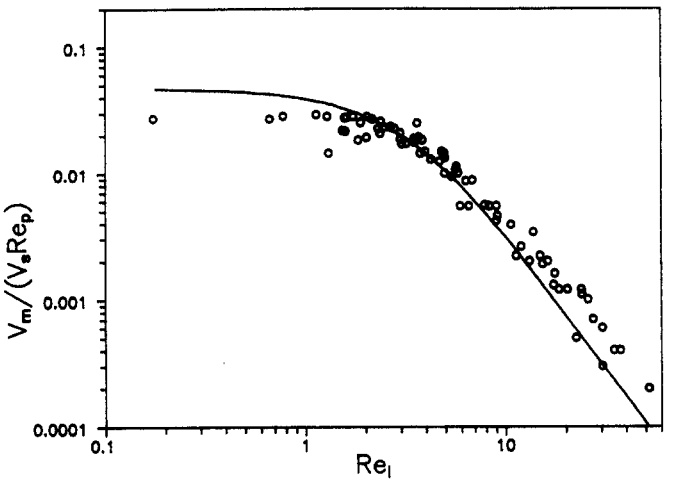

Figure 6. Plot of the ratio $V_m^{avg}/(V_s Re_p)$ vs Re_l.

Thus, it is evident that the rotation of the sphere does not play an important role in the lateral migration of the sphere.

4. CONCLUSION

Experimentally measured migration velocities [table 1 (a–f)] indicate that Vasseur & Cox's (1977) analysis predicts, fairly accurately, the migration velocity, and the dependence of the migration velocity on the distance from the wall up to an Re_p of 3.0. The errors are high when κ is 0.317, i.e. when the sphere is closest to the wall. This discrepancy can be seen in figure 6, where the measured migration velocities indicate that the asymptotic limit of $V_m(V_s Re_p)$ as $Re_l \to 0$, is lower than the value 3/64 as given by [15]. A similar observation was made by Vasseur & Cox (1977). Their theory assumes that the particle can be considered as a point force. This is a far-field approximation and implies that the distance l is very large as compared with the radius a. Hence this theory cannot be expected to accurately predict the force acting on the sphere when it is very close to the wall.

It was shown by Vasseur & Cox (1977) that a sphere sedimenting near a flat wall in a quiescent fluid does not rotate to $O(Re_p)$. This experimental study supports this observation. It was also observed that a sphere touching the wall does not migrate laterally as it sediments. However, in this case, the spheres did rotate as they sedimented. Experiments were also conducted in which the Re_p was in the range 5.0–10.0. It was observed that even at these Re_p values the spheres were expelled away from the wall as they sedimented. It was found that the agreement between the measured migration velocities and those predicted by [12] is poor (table 2) for this range of Re_p. Equation [12] is an $O(Re_p)$ expression, obtained by considering asymptotic expansions for velocity and pressure, and is strictly valid when $Re_p \ll 1$. Hence this expression cannot be expected to predict the force acting on the sphere at very high Re_p.

Table 2. Measured migration velocities and the migration velocities predicted by Vasseur & Cox's (1977) expression for high Re_p

κ	Dia (mm)	$\nu \times 10^{-4}$ (m^2/s)	Re_p	V_m^{exp}(mm/s): experimental	V_m(mm/s): Vasseur & Cox (1977) theory
0.31	0.2000	0.118	5.90	0.530	0.457
0.31	0.3175	0.118	9.33	0.530	0.348
0.21	0.2000	0.118	5.95	0.414	0.262
0.16	0.3175	0.118	9.34	0.189	0.097
0.13	0.3175	0.118	9.37	0.138	0.061
0.10	0.3000	0.092	5.76	0.072	0.038
0.09	0.2000	0.112	6.23	0.096	0.048
0.09	0.3175	0.118	9.39	0.078	0.029

The ratio V_m^{avg}/V_s was plotted vs Re_p for different values of κ for the range of Re_p from 0.1 to 10.0. The curves in figure 4 show the value of this ratio predicted by [12]. It can be seen that the agreement between the Vasseur & Cox (1977) theory and experimental observations is good up to an Re_p of 3.0. The theoretical predictions as well as experimental observations show that the ratio V_m/V_s passes through a maximum as Re_p increases and then decreases rapidly; this maximum occurs at $Re_p \simeq 1.0$.

The experiment described in section 2 involves the measurement of small distances. The most important factor which influences the error in the measured migration velocity is the error involved in measuring these distances. The maximum error which could have occurred in these measurements is roughly 0.1 mm. The migration velocity decays rapidly (in an inverse square manner) as the distance of the sedimenting sphere from the wall increases. Hence the largest error in the measured migration velocities can be expected for experiments for which $\kappa = 0.079$, and the maximum error in the measured migration velocities is approx. 10%.

Acknowledgement—This work was supported by the U.S. Department of Energy under Contract DE-FG02-88ER13919.

REFERENCES

BRETHERTON, F. P. 1962 The motion of rigid particles in a shear flow at low Reynolds number. *J. Fluid Mech.* **14,** 284–304.

COX, R. G. & BRENNER, H. 1968 The lateral migration of solid particles in Poiseuille flow: I. Theory *Chem. Engng Sci.* **23,** 147–173.

COX, R. G. & HSU, S. K. 1977 The lateral migration of solid particles in a laminar flow near a plane. *Int. J. Multiphase Flow* **3,** 201–222.

MCLAUGHLIN, J. B. 1989 Aerosol particle deposition in numerically simulated channel flow. *Phys. Fluids* **A1,** 1211–1224.

SAFFMAN, P. G. 1956 On the motion of small spheroidal particles in a viscous liquid. *J. Fluid Mech.* **1,** 540–553.

VASSEUR, P. & COX, R. G. 1977 The lateral migration of spherical particles sedimenting in a stagnant bounded fluid. *J. Fluid Mech.* **80,** 561–591.